Experimental analysis of FBG sensors thermal calibration under different loading conditions

Experimental analysis of FBG sensors thermal calibration under different loading conditions

Alessandro Aimasso
Department of Mechanical and Aerospace Engineering
Politecnico di Torino
Torino, Italy
alessandro.aimasso@polito.it

Giacomo Gallone
Department of Mechanical and Aerospace Engineering
Politecnico di Torino
Torino, Italy
giacomo.gallone@studenti.polito.it

Matteo D.L. Dalla Vedova
Department of Mechanical and Aerospace Engineering
Politecnico di Torino
Torino, Italy
matteo.dallavedova@polito.it

Paolo Maggiore
Department of Mechanical and Aerospace Engineering
Politecnico di Torino
Torino, Italy
paolo.maggiore@polito.it

***Abstract*—In recent decades, the use of the optical fiber has revolutionised several technological sectors, starting of course from communications. In addition to this field, however, its use has now become typical in even very different areas, from structural monitoring to medicine. This growth has largely been caused by the possibility of also using this technology for sensor applications. This aspect, together with its physical characteristics, has also led optical fiber to be appreciated in the aerospace sector. In particular, among the advantages there are the high sensitivity of optical sensors, the electrical passivity, the small cables' size and immunity to electromagnetic interference. Among the various optical fiber-based sensors, those used in the present work are the Fiber Bragg Gratings (FBG). They are realised by laser photoengraving directly into the fiber itself and they work like a filter. In fact, each FBG is able to reflect a specific wavelength, known as Bragg wavelength, which is proportional to the geometry of the sensor itself. In this way, it becomes possible to measure physical parameters acting on it, such as temperature, strain, etc. . The FBG function mechanism, however, generates only one optical output: in order to be able to distinguish the various contributions, a detailed knowledge of the proportionality between the reflected wavelength and the physical parameter considered is essential. The test campaign described in this work quantifies in detail the sensitivity of the FBG to temperature variation. More specifically, the sensor's thermal response is analysed as a function of the preload condition applied to the fiber. The results showed a variation of proportionality over the various measurement cycles. This leads to a twofold conclusion: on the one hand the need to carry out a specific calibration of the FBG in the case of pre-load; and on the other hand the possibility of exploiting this variation to decouple the thermal and mechanical contributions acting on the sensor.**

***Index Terms*—Optical fiber, FBG, thermal sensors, aerospace systems, monitoring.**

I. Introduction

The optical fiber is a structure with a cylindrical cross-section and it is made of glassy and polymeric materials. It consists of different concentric layers and its main characteristic is the ability of conducting light within itself [1]. The optical fiber has found wide use in many technological sectors, first and foremost in telecommunications (for transmitting optical signals over long distances), as well as in the medical and infrastructure sectors [2] [3]. However, the physical characteristics of optical fiber have also made it the subject of research for the aerospace sector [4] [5]. Among the most significant advantages there are the insensitivity to electromagnetic interference [6] (a condition typical of hostile environments and aerospace), the low cable's size, the high temperature operative range [7] and the electrical passivity. Moreover, a crucial aspect is the fact that optical fiber can also be used for sensor applications: in addition to the advantages already listed, it is also possible to have a large number of sensors on the same communication line, drastically reducing the overall footprint and the disturbance introduced [8]. This article focuses precisely on this aspect, analysing the calibration of FBG (Fibre Bragg Gratings) sensors. In particular, the trend of the sensor's thermal calibration curve is analysed, as a function of the pre-tensioning applied to the optical fiber. This is a functional analysis of the possibility of overcoming one of the main limitations of optical sensors, namely *cross sensitivity*. In fact, FBGs, have proven to be sensitive to several physical parameters simultaneously [9] [10], but since their output is solely optical, it is not always possible to distinguish the various physical contributions acting on it. Increasing the experimental data about the optical sensor response (to a thermal cycle under varying preload conditions) is the first step to define a standard process for decoupling the thermal and mechanical contributions acting on it.

II. Optical fiber and FBG sensors

The optical fiber is a glass and polymeric structure consisting of three concentric layers:

- core;
- cladding;
- coating.

The *core* is the innermost part of the fiber, it is made of glass and it has a diameter between 5 and 50 μm.
The *cladding* is a less pure glass and it is used to stem and to contain the light travelling in the core: this function is ensured thanks to a refractive index $n_2 < n_1$, obtained by doping the material on purpose. The thickness of this component is approximately 125 μm.
The optical fiber (core and cladding) then is surrounded by a polymeric material with a diameter of 200-250 μm, the *coating*, to increase the really low bending resistance of the fiber.
The principle governing the propagation of the light inside the fiber is the total reflection that occurs at the interface between core and cladding, characterised respectively by refractive indices n_1 and n_2 (with $n_2 < n_1$). This is quantified by the *Snell's Law*:

$$n_1 sin\theta_1 = n_2 sin\theta_2 \tag{1}$$

where θ_1 represents the angle of incidence formed between the light ray propagating in the core and the normal to the separation surface, while the angle of refraction θ_2 is formed between the normal and the light ray propagating in the cladding. The phenomenon of total reflection occurs when θ_2 exceeds the value of $\pi/2$. FBG sensors are obtained directly within the fibre by a process that involves the use of a laser capable of creating a periodic variation of the refractive index of the core (n_1): the result is a stretch of about 1 cm in which bands of material with a different refractive index are obtained arranged at a constant distance from each other, called *granting pitch* (Λ_G). Having defined the refractive index of the core as n_{eff}, when light passes through the Bragg grating, the FBG sensor reflects a particular wavelength called *Bragg frequency* λ_B defined by the equation:

$$\lambda_B = n_2 n_{eff} \tag{2}$$

Equation 2 demonstrates the dependence of the Bragg frequency on the grating pitch λ_G, i.e. on a distance: this means that a change in the reflected wavelength is to be attributed to a deformation in the grating generated by one or more external factors (mechanical deformation, thermal expansion, etc.). It is precisely this principle that underlies the fact that FBG sensors cannot separate a-priori the distinct physical contributions acting on it, as well described by the general equation governing an FBG:

$$\Delta\lambda_B = K_T \Delta T + K_\varepsilon \Delta\varepsilon \tag{3}$$

III. Experimental set-up

The optical fiber used in this test campaign was arranged as in the Fig. 2. It was attached to two metal supports using a resin, while in the sensor area it remained free suspended in the air. This choice was dictated by the desire to analyse only the performances of the sensor, eliminating the possibility of data being influenced by the material to which the sensor could be glued. In addition, one of the two plates is itself mounted on a micro-mover, whose movement applies a preload condition to the fiber. To apply the preload, the micro-mover's crank

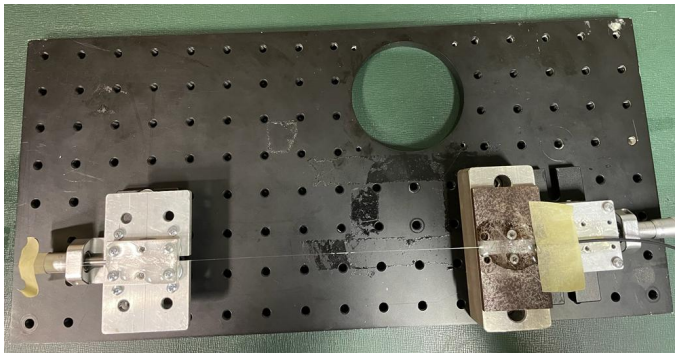

Fig. 1. The fiber used for the tests

shall be manually rotated. It is necessary that the resin allows the fiber to be permanently bonded to the micro-mover and the other support. A mixture consisting of *epoxy resin* and *hardener* in a $4:1$ ratio was used.
The *Climatic Chamber* is the instrument used to apply thermal cycles on the FBG sensor. The model adopted is the KK-50 CHLT manufactured by Kambic. The chamber could guarantee temperatures from -40 °C to 180 °C; in this work the range varied from 50 °C to -40 °C.
The *data acquisition system* consists of an optical interrogator connected to a computer. The *Interrogator* is a device capable of simultaneously emitting a light signal into the optical fiber and receiving the reflected wavelength from the Bragg gratings. The data are sent to the PC via LAN cable and saved on the PC as a text file (*.txt*). Data are sampled at a user-specified frequency between 2.5 HZ and 2.5 kHz. In this work, the maximum available frequency was used. Once the acquisitions have been completed, the data were processed using Matlab codes.
Finally, the temperature was monitored with the electronic *SHT85 sensor*. To correctly work, it was connected with an *ARDUINO UNO* breadboard, in turn linked to the PC via USB.

IV. Test campaign

The test campaign is based on five different tests respectively carried out with a specific level of preload imposed on the fiber. Each of them has two distinct phases: the *stabilization* and the *thermal cycling*.
The *stabilization* consists of a continuous acquisition of incoming data from the FBG and it is aimed at verifying that the imposed preload remains constant in time (i.e. that the resin is able to hold the fibre steady even under load). The desired preload is applied by rotating the micro-mover's crank and the setup is positioned on a flat and horizontal workbench. The fiber is then connected to the interrogator and data are monitored through the PC. The stabilization tests were all performed under the same environmental conditions: this allowed to compare the results between the different trials.
The *thermal cycle* in the climatic chamber constitutes the central part of each test. At first, the experimental set-up

is transferred inside the climatic chamber. Then, the system is brought to a temperature of 50 °C. Finally, applying a thermal rate of 30 °C/h, the optical instrumentation is placed at gradually decreasing temperatures until -40 °C is reached. In total, therefore, the thermal cycle lasts 3 hours. Of course, the test in climatic chamber can be carried out only if the stabilisation procedure has demonstrated sufficient stability for that particular pre-tension value.

A. *First cycle*

In this first test, no pre-load was imposed on the fiber, so it was not necessary to perform the stabilization cycle. Therefore, in this phase, we only take note of the wavelength at room temperature (always between 23 and 24 °C), which constitutes a reference to define future pre-tensioning (in terms of $\Delta\lambda_B$).

$$\lambda_{B_0} = 1555.029 \pm 0.001nm \tag{4}$$

At the end of the thermal cycle the FBG's characteristic curve $\lambda(T)$ (Fig. 2) is calculated: it results a piecewise linear calibration. In particular, a "knee" is observed around 0 °C, which marks the boundary zone between two curve sections characterized by different slopes (i.e., different temperature coefficients K_T):

- Above 0 °C, from linear interpolation it results $K_T = 0.0097$. Furthermore, it is also possible to find the intersection point of this straight section with the ordinate axis (the known term of the linear fit), which from a physical point of view represents the wavelength reflected by the fiber at 0 °C: $\lambda_0 = 1554.8112$ nm. This is a very reliable value because, considering the relationship (3) with the just-found K_T and ΔT = 23.0 °C (the temperature at which the reference wavelength was measured), we obtain:

$$\Delta\lambda_B = 0.0097 * 23.0 = 0.2231nm \tag{5}$$

  which means the reference wavelength with negligible error.
- Below 0 °C, a steeper curve section is observed, with $K_T = 0.0218$.

B. *Second cycle*

The second test was conducted on the fiber, this time pre-loaded, using the micro-mover crank that made a complete turn. Having applied a preload, the stability of the fiber needed to be verified for 60 minutes, at the end of which it was found that the pre-tension applied to the fiber is such that, at 23.1 °C:

$$\lambda_{B_1} \approx 1555.094 \pm 0.004nm \tag{6}$$

and therefore

$$\Delta\lambda = \lambda_{B_1} - \lambda_{B_0} \approx 0.061nm \tag{7}$$

At the end of the thermal cycle, the "knee" also appears in this case (Fig. 3), but it is found at T = 18 °C. In particular:

- for T >18 °C it results K_T = 0.0327;
- for T <18°C it results K_T = 0.0185.

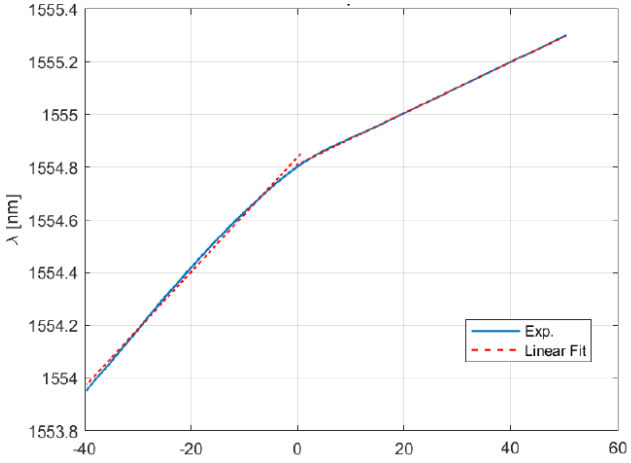

Fig. 2. Sensor calibration after thermal cycle 1

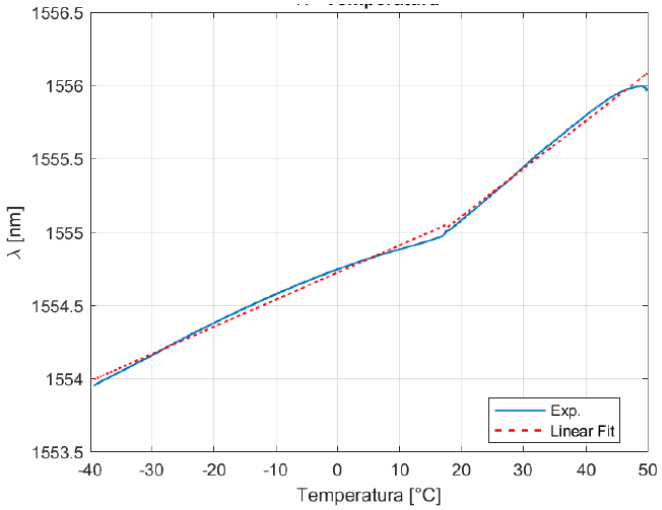

Fig. 3. Sensor calibration after thermal cycle 2

C. *Third cycle*

Starting from the previous test, the micro-mover crank was made to perform another half-turn (for a total of one and a half turns from the "discharged" position). The stabilization test of the fiber was carried out for 60 minutes, after which the acquisition was stopped. It can be stated that this pre-tension applied to the fiber is such that, at 23.9 °C:

$$\lambda_{B_2} \approx 1555.989 \pm 0.005nm \tag{8}$$

and therefore

$$\Delta\lambda = \lambda_{B_2} - \lambda_{B_0} \approx 0.960nm \tag{9}$$

Also in this situation, the well-known "knee" is found (Fig. 4) in the wavelength trend as a function of temperature; this appears at T = -16 °C. So, the temperature coefficients resulting from the linear fit are:

- for T >-16 °C it results K_T = 0.0371;
- for T <-16°C it results K_T = 0.0219.

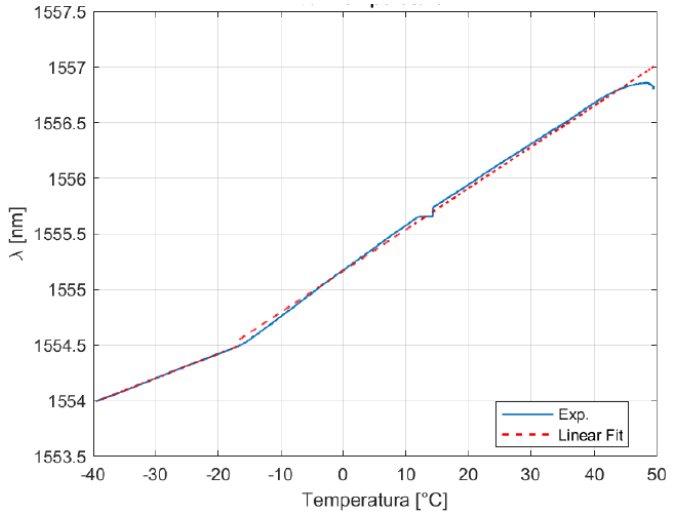

Fig. 4. Sensor calibration after thermal cycle 3

D. Fourth cycle

Starting from the previous test, the micro-mover crank was turned another half rotation (so a total of two complete rotations starting from the "discharged" position). The stabilization test of the fiber was successful again and lasted about an hour, after which the acquisition was stopped, as it was possible to proceed and carry out a thermal cycle. It can be stated that the pre-tension applied to the fiber is such that, at 23.7 °C:

$$\lambda_{B_3} \approx 1557.554 \pm 0.005nm \tag{10}$$

and therefore

$$\Delta\lambda = \lambda_{B_3} - \lambda_{B_0} \approx 2.525nm \tag{11}$$

In this case, the "knee" observed in all previous cases disappeared (Fig. 5), and the relationship between λ_B and temperature is represented by a straight line with a slope (temperature coefficient) K_T = 0.0414.

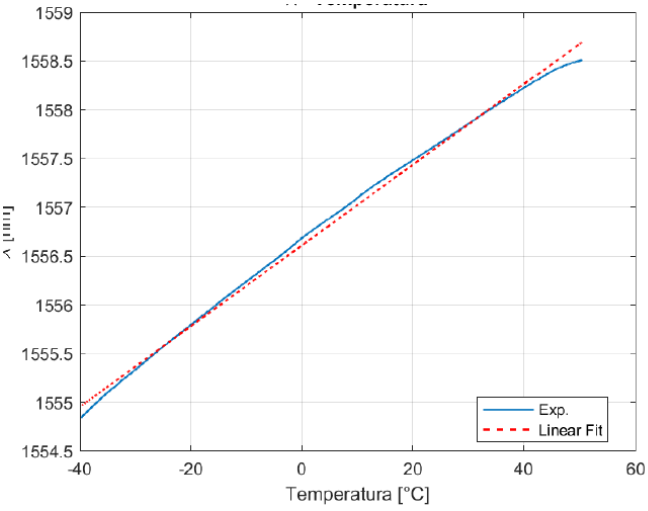

Fig. 5. Sensor calibration after thermal cycle 4

E. Fifth cycle

Starting from the previous test, the micro-mover crank was turned another half rotation (so a total of two and a half rotations starting from the "discharged" position). The stability of the fiber was verified for about an hour. It can be stated that this pre-tension applied to the fiber is such that, at 23.9 °C:

$$\lambda_{B_4} \approx 1559.074 \pm 0.004nm \tag{12}$$

and therefore

$$\Delta\lambda = \lambda_{B_4} - \lambda_{B_0} \approx 4.045nm \tag{13}$$

Even in this last test, the "knee" disappeared (Fig. 6), and the relationship between λ_B and temperature is represented by a straight line and a temperature coefficient (slope) K_T = 0.0421.

F. Sixth cycle

To carry out this test, the goal was to pretension the fiber in such a way that the wavelength at room temperature would be approximately equal to 1560 nm (about three and a third turns were made starting from the "unloaded" position).
The acquisition to verify the stability of the fiber was carried out for about an hour. However, it was evident from the beginning that the resin had yielded, and in fact, as shown in Fig. 7, during the acquisition time, λ_B remained anything but constant: it decreased by about 2 nm.
This test represents a point of no return: in fact, after verifying that the resin does not hold this pretension, it will no longer be possible to conduct tests of the same type with this FBG sensor, since trying to pretension it again in the same way will once again result in a decrease in wavelength exponentially.

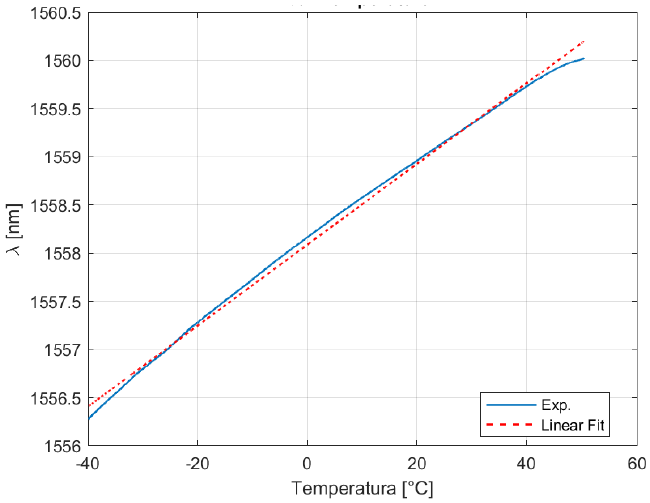

Fig. 6. Sensor calibration after thermal cycle 5

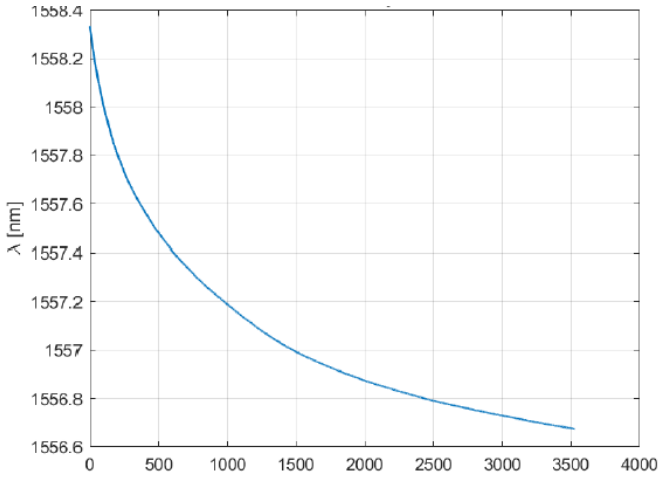

Fig. 7. Stabilization test output for cycle 6

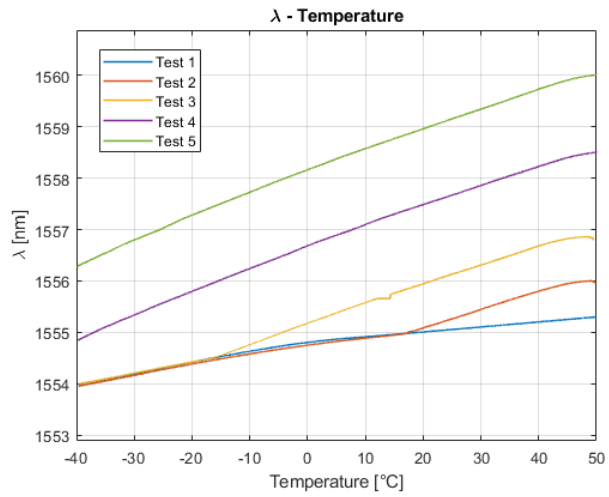

Fig. 8. Trends from not preloaded case (test 1) to maximum preload (test 5).

V. Results

Looking at the experimental results, the first aspect that can be observed is the non-complete linearity of the FBG's calibration curve. Furthermore, it is also evident that as the pre-loading varies, the calibration curve obtained is also different. In particular, a linear trend is observed in the first test (without any pre-load applied to the fiber), with a K_T defined above 0 °C and another, greater, below this value. The second test (the first with pre-tensioning applied) introduced a new slope change at around 20 °C, with a K_T significantly greater than the two previous ones. By increasing the pre-loading, at first (test 3) this change in slope is brought to lower temperature values (0 °C), while subsequently it no longer appears in the temperature range considered, leading to a linear relationship. The results obtained thus seem to indicate how the application of a preload changes the K_T coefficient of the thermal calibration curve. For low preload values, however, this variation can only be observed above a specific temperature, below which the trends coincide perfectly and the output value does not seem to be influenced by the preload. Furthermore, from the results obtained it is possible to parameterize λ_0 (i.e. the wavelength detected by the FBG at a temperature of 0 °C) as a function of the $\Delta\lambda$ induced by the preload. For not excessively low values of pre-loading, an approximately linear relationship is observed. Similarly, focusing on the temperature coefficients found in the various tests for temperatures greater than 20 °C (so that only one K_T value, that induced by tensioning, can be considered), it can be seen from Fig. 8 that the introduction of pre-tensioning significantly changes the K_T when compared to the unloaded fiber. However, while increasing the preload, in the subsequent tests the value tended to stabilize progressively (Fig. 10).

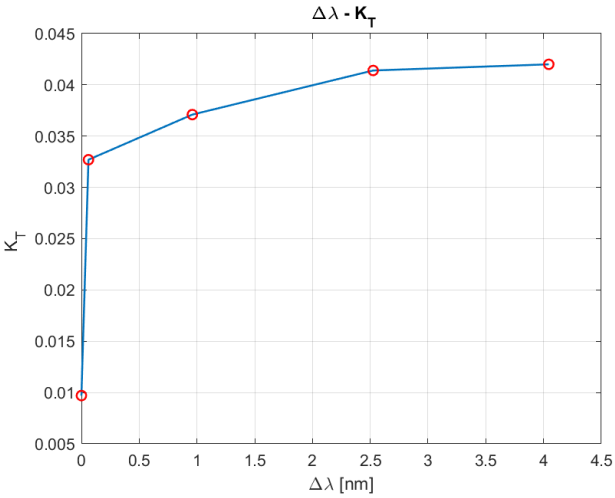

Fig. 9. Variation of K_T at different preloads.

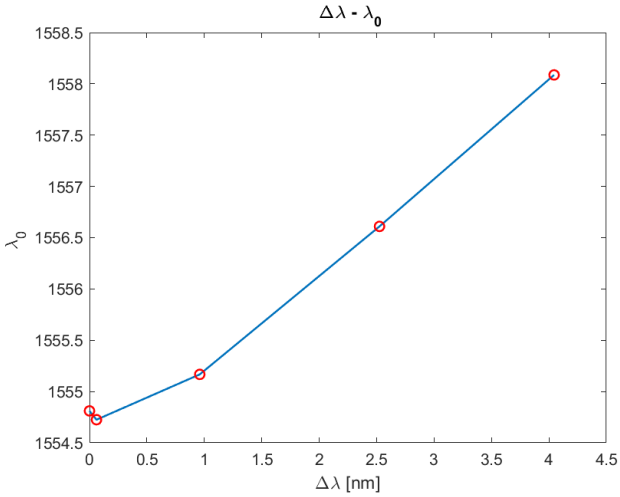

Fig. 10. Variation of λ_0 at different preloads.

VI. Conclusions

This work has produced positive and encouraging results. The possibility of having two FBG sensors with different K_T coefficients at the same temperature may represent a

first step toward the possibility of aperforming an accurate and automatic thermo-mechanical decoupling on the detected optical outputs. Furthermore, testing the effects of a fiber preload on the thermal sensitivity of FBG sensors expands the available experimenatl data about this technology.
The current results are then critical to define the best strategy for integrating optical sensors into the to-be-monitored aero-electro-mechanical systems, guaranteeing accurate measures.
Finally, from this work additional aspects that must be investigated in future activities are identified. At first, the test campaign must be repeated with closer pre-tensioning steps, increasing the number of tests. Furthermore, it is advisable to test the results under various environmental conditions. This could be accomplished, for example, by mounting the fibre on different materials and expanding the temperature range of the thermal cycle used. Finally, this trend must be validated under different heating conditions (for example, by heating only the sensor area rather than the entire experimental fibre/set-up).

ACKNOWLEDGMENT

Authors sincerely thanks FreMe project for the fundamental support in the work's conceptualisation, the Interdipartimental Research Centre PhotoNext for the instrumentation sharing and PNRR-NODES - Spoke 1 - Topic Aerospace for their support and excellent work.

REFERENCES

[1] Zhang, N.; Turk, S.; Davis, C.; Chiu,W.K.; Boilard, T.; Bernier, M. Fatigue Performance of Type I and Type II Fibre Bragg Gratings Fabricated by Femtosecond Laser Inscription through the Coating. Sensors 2022, 22, 8812.

[2] Ahuja D and Parande D 2012 Optical sensors and their applications J. Sci. Res. Rev. 1(5), 60–8.

[3] Kersey A D 1996 A review of recent developments in fiber optic sensor technology Optical Fiber Technology 291–317.

[4] Zhen Ma and Xiyuan Chen, "Fiber Bragg Gratings Sensors for Aircraft Wing Shape Measurement: Recent Applications and Technical Analysis", Sensors 19.1 (2019). url: https://www.mdpi.com/1424-8220/19/1/55.

[5] Mehrdad Pakmehr, Joannes Costa and Alireza Behbahani, Optical Exhaust Gas Temperature (EGT) Sensor and Instrumentation for Gas Turbine Engines, Conference: NATO STO Meeting: Transitioning Gas Turbine Instrumentation from Test Cells to On-Vehicle Applications STO-MP-AVT-306At: Athens, Greece, February 2019.

[6] Asep Andi Suryandi, Nur Sarma, Anees Mohammed, Vidyadhar Peesapati and Siniša Djurović, Fiber optic Fiber Bragg grating sensing for monitoring and testing of electric machinery: current state of art and outlook, Accepted for publication in MDPI Machines journal, November 2022.

[7] Wenyuan W, Yongqin Y, Youfu G and Xuejin L 2015 Measurements of thermo-optic coefficient of standard single mode fiber in large temperature range Proc. Int. Conf. Optical Instr. and Tech.: Optical Sensors and applications, 9620.

[8] Aimasso A., Vedova M.D.L.D., Maggiore P., Innovative sensor networks for massive distributed thermal measurements in space applications under different environmental testing conditions. (2022) IEEE 9th International Workshop on Metrology for AeroSpace, MetroAeroSpace 2022 - Proceedings, pp. 503 - 508.

[9] Aimasso A., Dalla Vedova M.D.L., Maggiore P., Quattrocchi G., Study of FBG-based optical sensors for thermal measurements in aerospace applications (2022) Journal of Physics: Conference Series, 2293 (1).

[10] Dalla Vedova M.D.L., Berri P.C., Aimasso A., Environmental sensitivity of Fiber Bragg Grating sensors for aerospace prognostics (2021), pp. 1561 - 1567, Proceedings of the 31st European Safety and Reliability Conference, ESREL 2021.